Re-assessing thermal response of schistosomiasis transmission risk: evidence for a higher thermal optimum than previously predicted

Ibrahim Halil Aslan [1, 2*], Andrew J. Chamberlin [2], Kaitlyn R. Mitchell [1, 2], Julie D. Pourtois [1, 2], Lorenzo Mari [3], Kamazima M. Lwiza [4], Chelsea L. Wood [5], Erin A. Mordecai [1, 6], Roseli Tuan [7], Raquel Gardini Sanches Palasio [8], Antônio M.V. Monteiro [9], Devin Kirk [1], Tejas S. Athni [1,10], Susanne H. Sokolow [1, 6], Eliezer K. N'Goran [11], Nana R. Diakite [11], Mamadou Ouattara [11], Marino Gatto [3], Renato Casagrandi [3], David C. Little [12], Reed W. Ozretich [12], Rachael Normal [13], Fiona Allan [14], Andrew S. Brierley [15], Ping Liu [4], Thiago A. Pereira [16], Giulio A. De Leo [1, 2]

[1] Department of Biology, Stanford University, Stanford, CA, USA
[2] Hopkins Marine Station, Stanford University, Pacific Grove, CA, USA
[3] Department of Electronics, Information and Bioengineering, Politeknik Milano, Milano, Italy
[4] School of Marine and Atmospheric Sciences Stony Brook University, New York, NY, USA
[5] School of Aquatic and Fishery Sciences, University of Washington, Seattle, WA, USA
[6] Woods Institute for the Environment, Stanford University, Stanford, CA, USA
[7] Pasteur Institute, São Paulo Health Public Office, São Paulo, SP, Brazil
[8] Department of Epidemiology, School of Public Health, University of São Paulo, São Paulo, SP, Brazil
[9] National Institute for Space Research, São José dos Campos, São Paulo, SP, Brazil
[10] Harvard Medical School, Boston, MA, USA
[11] Université Félix Houphouët-Boigny, 22 BP 770, Abidjan 22, Côte d'Ivoire
[12] Institute of Aquaculture, University of Stirling, Stirling, UK
[13] Computing Science and Mathematics, University of Stirling, Stirling, UK
[14] Department of Life Sciences, Natural History Museum, London, UK
[15] Scottish Oceans Institute, School of Biology, University of St. Andrews, St. Andrews, UK
[16] Institute for Stem Cell Biology and Regenerative Medicine, School of Medicine, Stanford University, Stanford, CA, USA
* Correspondence: iaslan@stanford.edu

Abstract: The geographical range of schistosomiasis is affected by the ecology of schistosome parasites and their obligate host snails, including their response to temperature. Previous models predicted schistosomiasis' thermal optimum at 21.7 °C, which is not compatible with the temperature in sub-Saharan regions where schistosomiasis is hyperendemic. We performed an extensive literature search for empirical data on the effect of temperature on physiological and epidemiological parameters regulating the free-living stages of *S. mansoni* and *S. haematobium* and of their obligate host snails, i.e., *Biomphalaria* spp. and *Bulinus* spp., respectively. We derived nonlinear thermal responses fitted on these data to parameterize a mechanistic, process-based model of schistosomiasis. We then re-cast the basic reproduction number, and prevalence of schistosome infection as functions of temperature. We found that the thermal optima for transmission of *S. mansoni* and *S. haematobium* range between 23.1-27.3°C and 23.6-27.9°C respectively. We also found that the thermal optimum shifts toward higher temperatures as the human water contact rate increases with temperatures. Our findings line up with an extensive dataset of schistosomiasis prevalence data in sub-Sharan Africa. The refined nonlinear thermal-response model developed here suggests a more suitable current climate and a greater risk of increased transmission with future warming.

Keywords: Schistosomiasis, Basic reproduction number, Mechanistic models, Climate Change, Thermal response

1. Introduction

The Earth's temperature has increased by approximately 0.6 degrees over the past 100 years and some climate change scenarios project even faster increases in the future [1–4], with potential impacts on ecosystems and human health. Temperature is one of the most important environmental determinants of the life history traits (LHT) of living organisms [2,5–8], especially ectotherms. Many of these ectotherms are then involved in the transmission of environmentally mediated diseases in humans, making transmission temperature-dependent [7]. In this work, we use a mechanistic, process-based epidemiological model to investigate the effect of temperature on the transmission risk of schistosomiasis, a water associated, acute and chronic parasitic disease of poverty, infecting more than two hundred million people per year, the vast majority in Sub-Saharan Africa (SSA) [9].

Schistosomiasis (also known as bilharzia or snail fever) is caused by parasitic flatworms of the genus *Schistosoma*. Of the five *Schistosoma* species of public health importance - *S. mansoni*, *S. haematobium*, *S. japonicum, S. intercalatum* and *S. mekongi* - most of the burden of schistosomiasis is caused by *S. mansoni*, endemic in both Africa and South America, and *S. haematobium,* endemic in Africa. These parasites have a complex life cycle that is heavily dependent on environmental conditions because the parasite life cycle depends on freshwater snail intermediate hosts and free-swimming *cercariae* that infect humans, both of which are ectotherms. In brief, humans with an active infection pass *Schistosoma* spp. eggs through their urine (*S. haematobium*) or stools (*S. mansoni*), and the eggs hatch upon water contact. The larvae, called *miracidia*, seek and infect freshwater host snails (of the genera *Bulinus* and *Biomphalaria* for *S. haematobium* and *S. mansoni*, respectively) and asexually reproduce in their tissue. A few weeks after infection, the infected snails start to shed a second free-living stage of the *Schistosoma* parasite, called cercaria. *Cercariae* infect people who contact the water by burrowing through their skin into their blood vessels. After a month, the parasites move in the blood plexus of the bladder (*S. haematobium*) or the small intestine (*S. mansoni*) where they reproduce sexually [10–13].

Temperature is a crucial driver at every stage of the schistosomiasis life cycle and affects different species of *Schistosoma* differently. The free-living stages (*cercariae* and *miracidia*) are directly impacted by water temperature. Effects of temperature have been reported for the survival and infectivity of *miracidia* [14–23], mortality rate of *cercariae* [16,24], *miracidia* hatching and cercarial emergence [25], snail fecundity, growth, mortality [9,26–28,28–32], and parasite incubation period within the snail [13,19,33,34], demonstrating pervasive effects of temperature across the schistosome life cycle. While these experiments provide insight on the response of individual LHTs, understanding the impact of temperature on the entire *Schistosoma* life cycle requires the integration of these LHTs across all life stages. Mathematical models [6,35,36] provide us with the flexibility and power to combine these LHTs and thereby predict how transmission and infection prevalence will be affected by temperature change.

Several mathematical models have been developed to examine the thermal response of schistosomiasis transmission [25,37–39]. However, these models are typically limited to a particular life stage of the parasites [25] or omit the temperature dependence of important LHTs [37,39]. For example, the model presented in [40] and later used by [25] does not include the prepatent period in snails, which is strongly correlated with temperature. In addition, the difference in temperature response between *S. mansoni* and *S. haematobium* [13,19,33] has not always been considered in previous studies [25,37,39,41,42]. Thus, we still lack a comprehensive understanding of the impact of temperature on schistosomiasis transmission that fully accounts for its complex life cycle and differences between *Schistosoma* species.

We developed a comprehensive thermal-sensitive mechanistic model of schistosomiasis and tested its performance across SSA using data from the Global Neglected Tropical Disease (GNTD) database. The temperature-dependent parameters used in the model are based on thermal performance curves (TPCs) that were fitted separately to empirical data for *S. mansoni* and *S. haematobium* to account for their unique LHTs. The species-specific thermal responses of the basic reproduction number for schistosomiasis (R_0) and the prevalence of infection in humans were calculated for *S. mansoni* and *S. haematobium* to measure the intensity of transmission with respect to temperature. We then identified the most critical temperatures, the confidence intervals around the R_0 and the prevalence curves for both parasites and analyzed the impact of human water contact behavior on thermal response of schistosomiasis. Finally, we compared our estimates with previous estimates of the optimal temperature for schistosomiasis transmission by using the data from the GNTD database. We show that the thermal response of R_0 and the prevalence in humans are unimodal curves and their optimal temperatures are higher than previously determined. In addition, we found that human water contact rate shifts this optimal temperature to a higher degree.

2. Materials and Methods

Model description

We used a system of ordinary differential equations (ODEs) with temperature-dependent parameters to formulate a mechanistic model of schistosomiasis transmission. The model consists of three compartments for snails and two compartments for worms inside the human body (**Figure 1**): susceptible snails (S); prepatent snails, infected by *miracidia* but not shedding *cercariae* yet, which is also the stage of developing sporocysts [43] (P); infectious snails, shedding *cercariae* (I); mean number of immature worms that do not produce eggs (W); and mean number of mature worms that produce eggs (W_m).

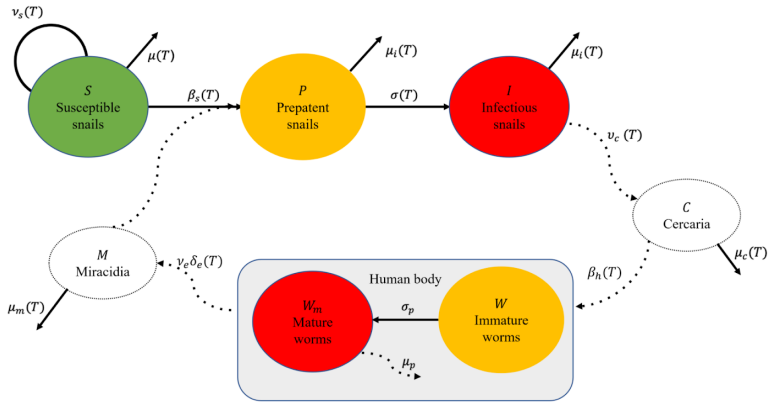

Figure 1: The transmission of schistosomiasis requires infection of a susceptible snail by free-living *miracidia* and the subsequent release of *cercariae* in the water after a prepatent period. *Cercariae* can infect humans, where they become mature worms and produce eggs. Eggs are then released from the human body through urine or stool and later hatch and become *miracidia*, thus completing the parasite's life cycle. Processes whose dynamics are considered explicitly are shown with a solid arrow, while processes for which quasi-equilibrium is assumed are depicted with a dashed arrow. We highlight uninfected compartments with green, infected compartments with red, and incubation periods with yellow.

The dynamics of free living *cercariae* (C) and *miracidia* (M) are considered implicitly: the lifespan of *miracidia* and *cercariae* is short [14–16,24] (i.e., less than 1 day) with respect to the lifespan of snails and adult parasites; we therefore embedded their faster dynamics into the slower dynamics of the rest of the model by assuming that the abundances of the larval stages are at quasi-equilibrium with the other state variables for a given temperature, that is

$$M^* = \frac{h\nu_e\delta_e(T)}{\mu_m(T)}W_m \quad (1)$$

$$C^* = \frac{\nu_c(T)}{\mu_c(T)}I \quad (2)$$

where T is temperature, h is the human population size (assumed constant), ν_e is the number of eggs produced daily by a mature worm, $\delta_e(T)$ is the probability that eggs successfully hatch into *miracidia*, $\mu_m(T)$ is the mortality rate of *miracidia*, $\nu_c(T)$ is the per-capita daily cercarial shedding rate, and $\mu_c(T)$ is the mortality rate of *cercariae* (see Figure 1-9 in Supplementary Materials (SM)). The model describing schistosomiasis dynamics is thus represented by the following set of ODEs:

$$\frac{dS}{dt} = (\nu_s(T) - \nu(S+P+I))(S+rP) - \lambda(T)S - \mu(T)S \quad (3)$$

$$\frac{dP}{dt} = \lambda(T)S - (\sigma_s(T) + \mu_i(T))P \quad (4)$$

$$\frac{dI}{dt} = \sigma_s(T)P - \mu_i(T)I \quad (5)$$

$$\frac{dW}{dt} = C_w(T)\beta_h(T)C^* - \sigma_p W \quad (6)$$

$$\frac{dW_m}{dt} = \sigma_p W - (\mu_h + \mu_p)W_m \quad (7)$$

Snails reproduce at the per-capita rate $\nu_s(T)$, reduced by $\nu \cdot (S+P+I)$ to account for (logistic-like) density-dependent competition among snails (Eq. 3). The fecundity of infected but not infectious (i.e., prepatent) snails is reduced by a factor r due to the infection, whereas snails in the compartment I do not reproduce [44]. Following [45], the per-capita force of infection $\lambda(T)$, i.e., the rate at which susceptible snails become infected, is assumed to be an increasing and saturating function of the number of *miracidia* M^* relative to that of snails $N = S + P + I$, namely:

$$\lambda(T,t) = \Lambda\left(1 - e^{-\beta_s(T)\frac{M^*}{N}}\right) \quad (8)$$

where Λ is the maximum force of infection and $\beta_s(T)$ is the transmission rate from *miracidia* to snails. Uninfected snails die at a per-capita rate $\mu(T)$. Prepatent snails become infectious at a rate $\sigma_S(T)$, and prepatent and infectious snails both die at a rate $\mu_i(T)$ (Eq. 4 & 5). $\beta_h(T)$ is the probability of parasites establishing at which new infections are acquired in the human compartment (Eq. 6). $C_w(T)$ modulates the human contact rate with water in response to temperature, following observations that the frequency and duration of contact with waters are higher at higher temperatures [46]. Finally, worms mature at a rate σ_p and die at a rate $\mu_p + \mu_h$, where μ_h represents the death rate of the human host and μ_p is the mortality rate of the worm itself (Eq. 7). The maturation rate of the parasite, σ_p, the egg production rate, ν_e, and the death rates of worms, μ_p, do not depend on external temperatures because these life stages occur in the human body at a fixed temperature. The human mortality rate, μ_h, is also assumed to be independent of temperature.

Model Parameterization

We conducted a literature review of peer-reviewed papers reporting empirical data on thermal sensitive model parameters derived from laboratory experiments. We restricted our search to experiments and data for *S. mansoni* and *S. haematobium* parasites, and on snails of the genus *Biomphalaria* and *Bulinus* spp. respectively, without any time or geographical constraint. When necessary, demographic rates were converted to the same unit of our model (see SM) and the data regarding transmission rates $\beta_s(T), \beta_h(T)$ also converted to the unit of our model by using an SIR type model (SM). For each demographic and epidemiological thermal sensitive parameter, we compounded the data collected from multiple empirical studies (when available) and estimated the best fitting curve with the R package rTPC (Padfield and O'Sullivan) [47]. rTPC was specifically developed to fit a family of 24 TPCs previously described in the literature (e.g., quadratic, Brière, Gaussian) using non-linear least squares regression. This R package requires at least 7 data points to fit the family of 24 curves. Based on the Akaike Information Criterion (AIC) and expected qualitative shape of the thermal performance curves, we determined the best-fitting curve for each temperature-dependent parameter. TPCs were estimated separately for *S. mansoni* and *S. haematobium*, as well as for *Biomphalaria* and *Bulinus* spp. To determine the uncertainty around each TPC, we used a bootstrap resampling method to construct 95% confidence intervals by using the R package of thermal performance curves by Daniel Padfield [47]. Results of the bootstrap resampling are shown with figures in the SM. Temperature-invariant parameters were estimated from the literature [11,37,48]. The human population abundance h was set to 1,000 people, and the parameters ν, Λ were fit so that prevalence of infection in snails is around 5%, as documented by [11] and other field studies in the lower basin of the Senegal river [48–50]. In addition, we adjusted these parameters to set the MPB in the human population to 80%, as described in [42].

While it is expected that frequency and duration of human contact with water may increase with temperature, there is a paucity of rigorous empirical studies systematically reporting field observations useful to estimate water contact rate as a function of temperature, as documented for instance in [46]. For these reasons, we first ran simulations assuming that the relative contact rate with water $C_w(T)$ is constant and equals to 1 and then derived the thermal envelope and the thermal optima. Second, we ran a further set of simulations assuming that the contact rate is an increasing and saturating function of temperature that levels off when temperature is above 30 °C, namely:

$$C_w(T) = \frac{1}{1+e^{-a(T-T_{med})}} + b \qquad (9)$$

where:

- $b \geq 0$ is the minimum contact rate at low temperature
- T_{med} is the temperature at which the slope of mid-point occurs
- $a \geq 0$ is the parameter that governs the steepness of the function.

This curve was qualitatively parameterized by using field observations reported by Sow et al. (2011) [46].

Basic reproduction number R_0 and prevalence in human

The basic reproduction number R_0 is the number of new infections caused by one infectious case in a fully susceptible population [51] and is generally used to determine the stability of the disease-free equilibrium (DFE) [35]. If $R_0 < 1$, the DFE is stable and the disease is not able to invade and establish in the population; otherwise, the DFE is unstable, the disease is able to establish in the population, and the number of infected snails and the MPB in the human population may converge toward a non-trivial (i.e., strictly positive), long-term equilibrium. Note that we are only considering parameter sets in here for which the global extinction equilibrium is asymptotically unstable. We derived the basic reproduction number R_0 by using the next generation matrix method [51,52] (see SM for detail).

$$R_0(T) = \left(\frac{\Lambda \beta_s(T) h \delta_e(T) v_e \beta_h(T) v_c(T) \sigma_s(T)}{\mu_m(T)(\mu_h + \mu_p)\mu_c(T)\mu_i(T)(\sigma_s(T) + \mu_i(T))} \right)^{1/2} \quad (10)$$

where the parameters are either constant or a function of temperature T. We also derived the disease-free equilibrium as

$$(S^*, P^*, I^*, W^*, W_m^*,) = \left(\frac{v_s(T) - \mu(T)}{v}, 0, 0, 0, 0 \right) \quad (11)$$

The basic reproduction number R_0 is particularly useful to assess how likely a disease is to invade a fully susceptible population. Therefore, it is interesting to estimate not only its thermal optimum but also its thermal breadth. On the other hand, schistosomiasis is also a chronic disease with the adult parasite able to live for years in the human body. Therefore, it is also interesting to assess the relationship between temperature and the MPB at the endemic equilibrium. Accordingly, we simulated disease dynamics until the model reached the endemic equilibrium, and, under the common assumption of a negative binomial distribution of the adult parasites in the human population [53], we used the mean parasite burden at equilibrium to derive the prevalence of infection in the human population as a function of temperature. We assume the probability of one or more pairs of worms represents the prevalence of infection in humans.

Model comparison with prevalence data

We used the GNTD database to evaluate whether our model results are consistent with the prevalence data observed in the field. The 2015 version of the GNTD database included over 11,000 data points of schistosomiasis prevalence in the human population from nearly 8,000 unique locations. We limited our analysis to locations with non-zero prevalence, as our model parameterization assumes schistosomiasis is present in the population. We then used quantile regressions to investigate whether the R_0 estimates obtained from our model performed better or worse as a predictor for reported prevalence than the estimates from the thermal sensitive model presented in [25]. Models were compared using AIC. For ease of visualization, we created bins made of 400 data points and the 98th percentile of the bins shown in **Error! Reference source not found.**. Details about the models and visualizations of the raw dataset are available in the SM.

Parameter sensitivity analysis

We conducted a sensitivity analysis to discern the impact of each parameter on the disease transmission dynamics. Briefly, we derived the partial derivative of R_0 with respect to temperature, while holding all other parameters constant except for the parameter of interest (details provided in SM). In addition, we analyzed how much the thermal response of each demographic and epidemiological parameter influences model outcomes by deriving the thermal response of R_0 while keeping the parameter of interest constant.

3. Results

Thermal performance of model parameters

TPCs were fitted for each temperature-dependent parameter in model (1-9). Data and best-fit curves are shown in **Error! Reference source not found.** (see SM for confidence intervals) and summarized in **Table 1**. Specifically, TPCs were estimated for snail fecundity rate, natural mortality, additional mortality caused by infection, and incubation period for *Biomphalaria* and *Bulinus* spp. separately. TPCs for the cercarial shedding rate in snails were only fitted to data for *Biomphalaria* spp., as we could not find similar studies for *Bulinus* spp. TPCs for the mortality rate of *miracidia* and the duration of the prepatent phase were fitted separately for *S. mansoni* and *S. haematobium*, whereas TPCs for the probability of *cercariae* successfully infecting the human host, probability of *miracidia* hatching success, and mortality rate of cercarial were only fitted to data for *S. mansoni*.

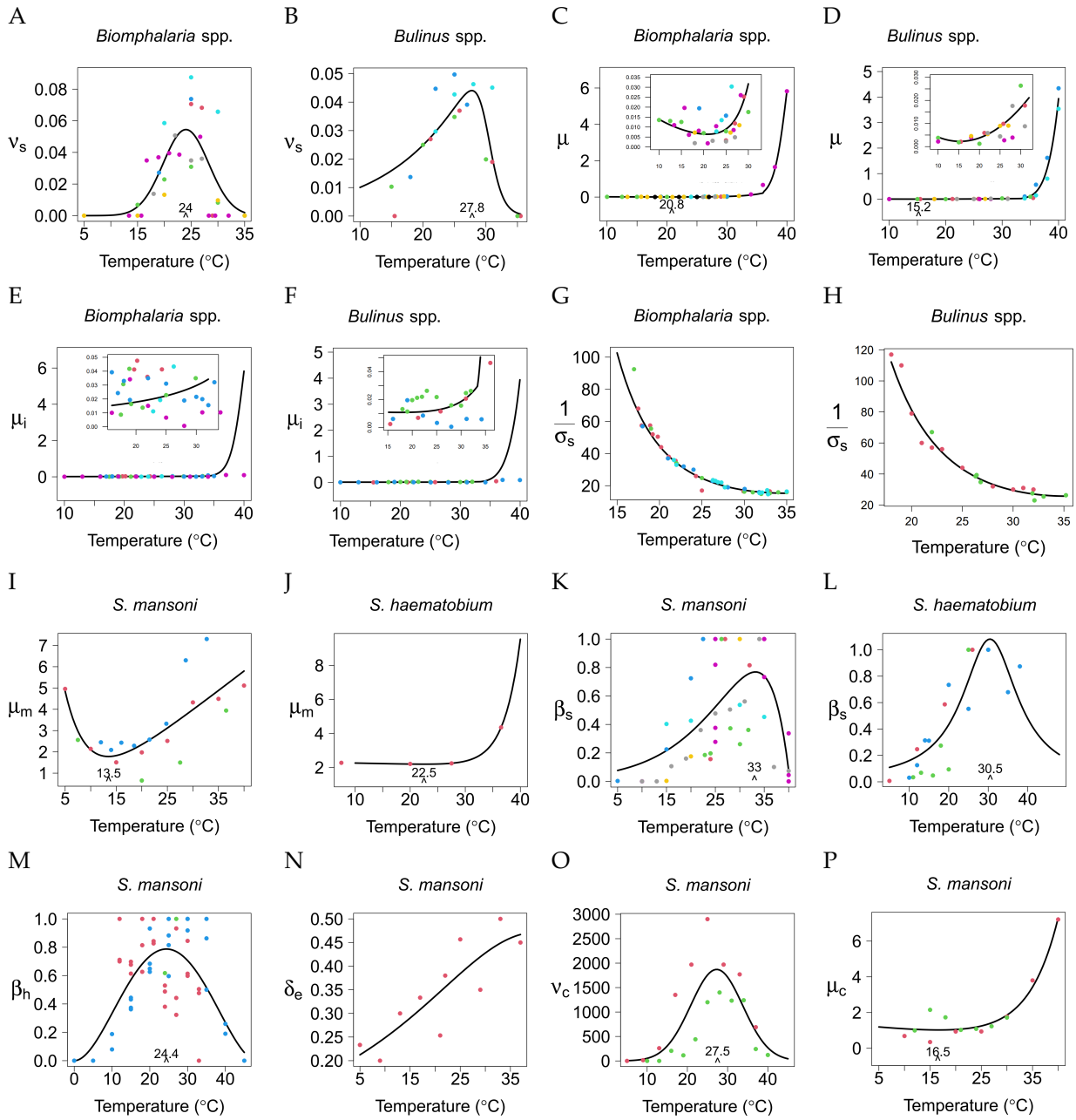

Figure 2 : Thermal performance curves for temperature-dependent parameters. Inset panels show the thermal curve for a subset of temperatures on a zoomed-in y-axis. Different colors are used for different data sources.

We used the Euler-Lotka equation to derive the fecundity rate of *Biomphalaria* and *Bulinus* snails (**Error! Reference source not found.**A and B), respectively, from snails' egg laying, hatching, survival, and maturation rates (SM). Separate thermal curves for each of these processes are available in the SM. We found the best-fit function for fecundity rate for *Biomphalaria* spp. (*B. pfeifferi, B. alexandrina, B. glabrata, B. sudanica* is a concave unimodal shape that peaks at 24 ◦C, with lower (T_{min}) and upper (T_{max}) critical thermal thresholds at ~14 and 33°C, respectively. On the other hand, the best fit for *Bulinus* spp. (*B. globosus, B. truncatus, B. nyassanus*) fecundity data is a Johnson Lewin curve with a peak close to 28 ◦ T_{min} ,T_{max} around 10 and 32 ◦C, respectively. These peak temperatures are higher than the previous estimate (22.1 ◦ C) for all *Biomphalaria* and *Bulinus* spp. combined. Overall, we found *Bulinus* spp. to have a lower fecundity rate than *Biomphalaria* spp., with *Biomphalaria alexandrina* having the lowest fecundity rate among *Biomphalaria* spp. (see SM). We also observed that the confidence interval around the fecundity rate TPC for *Biomphalaria* spp. is narrower than for *Bulinus* spp. (Figure S1B-S2B).

The mortality rates of snails (**Error! Reference source not found.**C and 2D) are calculated from the fraction of snail surviving during each laboratory experiment at a given temperature. The best fit for *Biomphalaria* spp. (*B. pfeifferi, B. alexandrina, B. sudanica*) is a unimodal convex curve (Spain) [55] with a minimum at 21 ◦C. The best fit for *Bulinus* spp. (*B. globosus, B. truncatus, B. africanus, B. nyassanus*) is a quadratic function [56] with a minimum close to 15 ◦C. The empirical data show that mortality increases rapidly at high temperatures. The best fit across the entire temperature range accounted for in this study was obtained by using two curves, one for temperatures below 33 ◦C (**Error! Reference source not found.**C and D, inset panels) and the other for temperatures above 33 ◦C. We observed lower variability for *Biomphalaria* spp. than *Bulinus* spp. in the confidence intervals around the TPC for the snail's mortality rate (Figure S3B-S4B).

The mortality rates of infected snails were calculated from the snails' survival time at different temperatures after exposure to *miracidia* (**Error! Reference source not found.**E and 2F). The best-fit curves for *Biomphalaria* spp. (*B. glabrata, B. pfeifferi*) and *Bulinus* spp. (*B. globosus, B. truncatus*) are Flinn [57] and Spain [55], respectively. Mortality rates increase as temperature increases both for *Biomphalaria* spp. infected with *S. mansoni* and for *Bulinus* spp. infected with *S. haematobium*. As for the natural mortality rate of snails, we fitted the curves for mortality rate iof infected snails to data for higher and lower temperatures separately (**Error! Reference source not found.**E and 2F inset panels). We observe strong noise in the data, particularly for *Biomphalaria* spp., and wider confidence intervals at higher temperatures (Figure S12B-S13B).

The prepatent period, the average time between snail infection with *miracidia* and the onset of cercarial shedding (**Error! Reference source not found.**G and H), is best fit by a declining tail of a Gaussian function of temperature for both *Biomphalaria* spp. (*B. glabrata, B. pfeifferi*) and *Bulinus* spp. (*B. truncatus, B. globosus*) (Figure S5B-S6B) [58]. Data show little variability in prepatent time among snails of the same genus, and that *Bulinus* snails have a longer prepatent time than *Biomphalaria* snails (**Error! Reference source not found.**G and H).

The mortality rate of *miracidia* is calculated from their survival time at different temperatures (**Error! Reference source not found.**I and J). The best-fit curve is Thomas [59] for *S. mansoni*, with the lowest mortality rate at 13.5 ◦C, and Spain [55] for *S.haematobium*, with the lowest mortality rate occurring at 22.5 ◦C. We found strong noise in the confidence interval around the TPC at high and low temperatures for *S. mansoni*. We could not calculate the confidence intervals around the TPC of *S. haematobium* through bootstrapping due to the small size of the dataset. In this case, we generated a confidence interval by resampling from the confidence interval of the estimated TPC parameters. The mortality rate of *cercariae* (**Error! Reference source not found.**P) is also calculated from the proportion of surviving larvae at different temperatures. The best-fit curve for the data is Spain [55], with the lowest mortality of *cercariae* at 16.5 ◦C. We observe a rapid increase at high temperatures, with narrow confidence intervals around TPC (Figure S9B-S10B-S11B).

The transmission rate from *miracidia* to snails (**Error! Reference source not found.**K and L) was estimated by utilizing a mechanistic model from data on the percentage of infected *Biomphalaria* spp. (*B. glabrata, B. pfeifferi*) and *Bulinus* spp. (*B. globosus, B. trancatus*) following exposure to *S. mansoni* and *S. haematobium* respectively (see SM). The best-fit curves are Spain [55] for *Biomphalaria* spp. exposed to *S. mansoni* and Flinn [57] for *Bulinus* spp. exposed to *S. haematobium*. Transmission rate peaked at 33 ◦C for *Biomphalaria* spp. and 30.5 ◦C for *Bulinus* spp. The transmission rate from *cercariae* to humans (**Error! Reference source not found.**M) is estimated from a separate SIR model of mice and cercaria by using the data of infection rate. Experimental studies are only available for *S. mansoni.* The best-fit function for this data is a Brière curve [60], with an optimal temperature for transmission around 24.5 ◦C. We observe transmission happening at as low as 10 ◦C and as high as 40 ◦C. Due to different laboratory conditions, both the miracidium-to-snail and the cercaria-to-human transmission rates have strong noise in the data and wide confidence intervals (Figure S14B-S15B-S16B).

The hatching probability of *miracidia* (**Error! Reference source not found.**N) is evaluated as the proportion of *miracidia* successfully hatching. Only one study was found measuring this parameter and it focused on *S. mansoni*. The best-fit function for these data is Flinn [57], showing a monotonic increase with temperature. Uncertainty increases with temperature (Figure S7B). The number of *cercariae* released per day by one snail (**Error! Reference source not found.**O) was obtained from two empirical studies of *Biomphalaria* spp. infected by *S. mansoni*. Based on these two studies, the best-fit function is a Gaussian curve [58], with its peak at 27.5 ◦C, matching finding in [25], and T_{min}, T_{max} are 10 and 40 ◦C, respectively. The confidence interval around the TPC becomes wider at higher temperatures (Figure S8B).

Table 1: Summary of temperature-dependent parameter shows the shape of curve, resources of data, location in the figure panel and optimal temperature with 95 percent credible interval for each corresponding parameter.

Parameter	Species	Shape	References	Figure Panel	Optimal Temp. (95% CI)
Snails' fecundity rate $\nu_s(T)$	*Biomphalaria* spp.	Unimodal Concave	[26–28,31,61,62]	A	24 ◦C (22.87, 25.60) ◦C
	Bulinus spp.	Unimodal Concave	[9,27,32,62]	B	27.8 ◦C (25.56, 30.32) ◦C
Snails' mortality rate $\mu(T)$	*Biomphalaria* spp.	Unimodal Convex	[19,26–28,30,61,63]	C	21 ◦C (17.8, 23.5) ◦C
	Bulinus spp.	Unimodal Convex	[9,27,30,32,63,64]	D	15 ◦C (10, 19) ◦C
Infected snails' mortality rate $\mu_i(T)$	*Biomphalaria* spp.	Increasing	[19,23,33,34]	E	NA
	Bulinus spp.	Increasing	[9,18,65]	F	NA
Snails' prepatent period $\sigma_S(T)$	*Biomphalaria* spp.	Decreasing	[13,19,33,34]	G	NA
	Bulinus spp.	Decreasing	[13,65]	H	NA
Miracidia's mortality rate $\mu_m(T)$	*S. mansoni*	Unimodal Convex	[14–16]	I	13.5 ◦C (11.36, 18.08) ◦C
	S. haematobium	Unimodal Convex	[15]	J	22.5 ◦C Insufficient data
The transmission rate of schistosomiasis in the snails $\beta_s(T)$	*S. mansoni*	Unimodal Concave	[14,15,19–23]	K	33 ◦C (31.51, 34.34) ◦C
	S. haematobium	Unimodal Concave	[15,17,18]	L	30 ◦C (28.33, 33) ◦C
The transmission rate of schistosomiasis in humans $\beta_h(T)$	*S. mansoni*	Unimodal Concave	[16,20,21]	M	24.4 ◦C (22.27, 26.81) ◦C
The Probability of hatching success of *miracidia* $\delta_e(T)$	*S. mansoni*	Increasing	[25]	N	NA

The number of cercariae released $\nu_c(T)$	*Biomphalaria* spp.	Unimodal Concave	[23,25]	O	27 ◦C (25.15, 31.10) ◦C
The mortality rate of the cercaria $\mu_c(T)$	*S. mansoni*	Unimodal Convex	[16,24]	P	16.5 ◦C (10, 21.81) ◦C

Thermal response of R_0 and prevalence in humans

To investigate how transmission intensity varies with temperature, we calculated the basic reproduction number R_0 and prevalence of schistosomiasis in humans as discussed in the Methods section. We found that the thermal response curve of R_0 is a unimodal concave shape for both *S. mansoni* and *S. haematobium*, peaking at 25.5 ◦C (CI: 23.1-27.3 ◦C) and 26.2 ◦C (CI: 23.6-27.9 ◦C) with 3.68 and 3.44 peak value, respectively (**Error! Reference source not found.**A-B). The thermal response of the prevalence in humans also has a concave shape for both *S. mansoni* and *S. haematobium*, with peaks at 24 ◦C (CI: 23.1-27.3 ◦C) for *S. mansoni* and 26 ◦C (23.35-27.5 ◦C) for *S. haematobium* (**Error! Reference source not found.**C-D).

We compared the ability of our R_0 thermal curve to predict GNTD prevalence data with previous R_0 estimate (as previous models did not estimate prevalence directly). Using a quantile regression, we found our R_0 estimate to be a significant predictor of median prevalence, while the previous R_0 by *[25]* estimate was not ($p < 0.01$ and $p = 0.3$, respectively). These results were consistent for other quantiles (see SM).

A

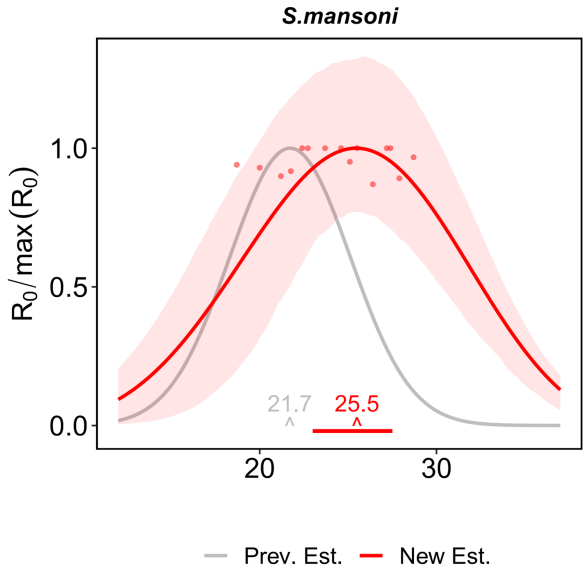

B

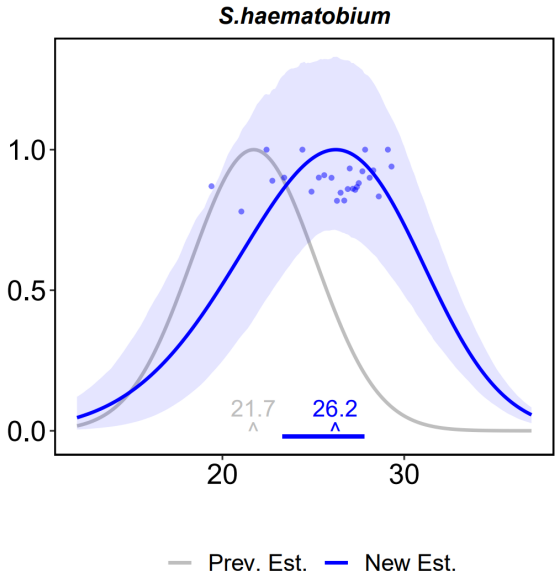

C

D

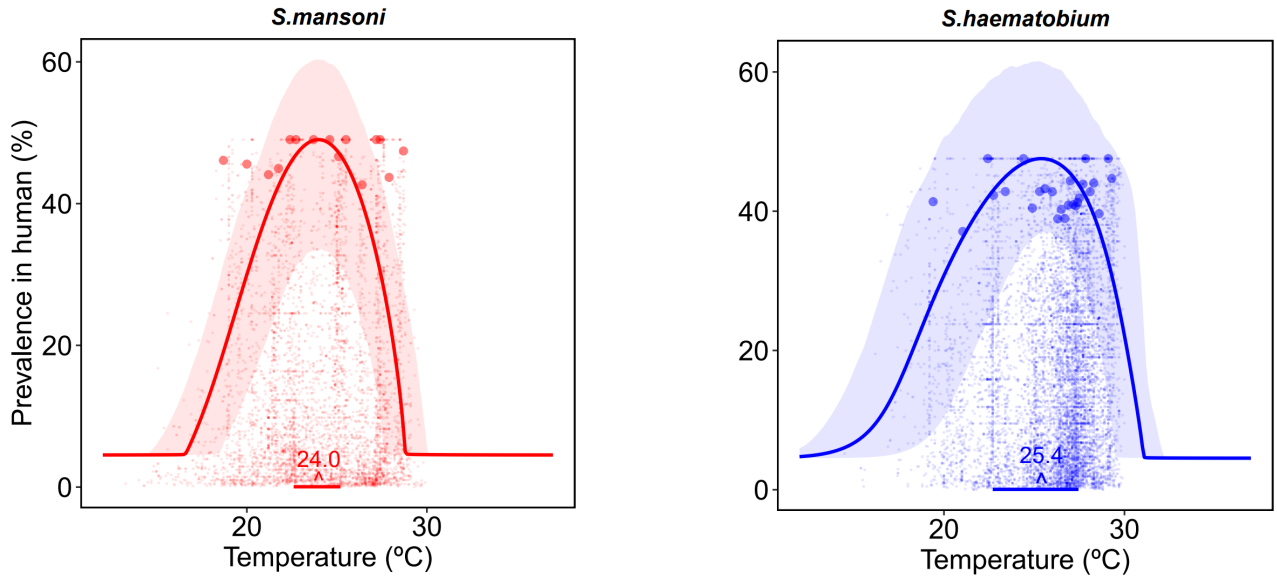

Figure 3: Thermal response curve of disease transmission (R_0) (A and B) and prevalence of schistosomiasis in humans (C and D) for *S. mansoni* (A and C) and *S. haematobium* (B and D), with 95th percentile of prevalence data from the GNTD database. We normalize the thermal response curve of R_0 and prevalence data by their maximum values. The shaded area around the curves are the confidence interval for the TPCs obtained from bootstrap resampling and the shaded points in C and D are the actual data of GNTD. The gray curve shown in A and B is the previous estimation by *[25]*. Horizontal lines at the bottom show the 95 percent confidence interval of the thermal optimum.

Parameter sensitivity of R_0

We performed a sensitivity analysis of R_0 with respect to each parameter (**Figure 4**A-B). We found that several demographic and epidemiological parameters have similar impact around the optimal temperature. However, at lower temperatures, $\nu_c(T)$ and $\mu_m(T)$ have the highest positive and negative impact, respectively, whereas, at the high temperatures $\beta_s(T)$ and $\mu_c(T)$ have the highest positive and negative impact, respectively, on the per-capita of R_0.

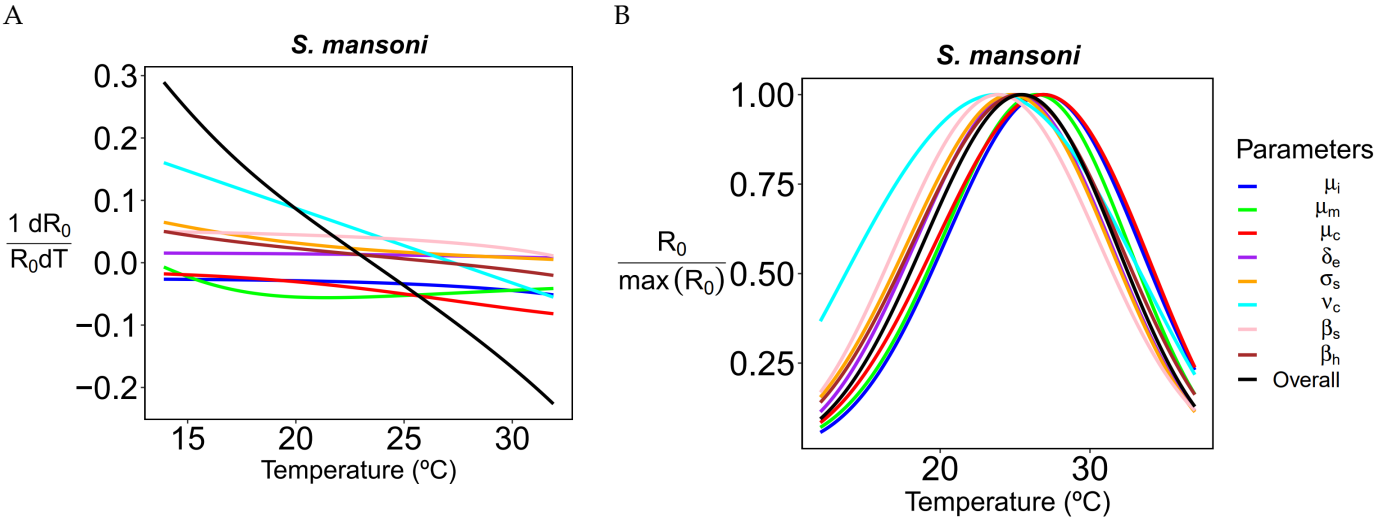

Figure 4: The plot on the left side (A) shows the derivative of R_0 with respect to temperature per unit of R_0while assuming all parameters (except the focal one) are constant for different values of reference temperature . The plot on the right side (B) shows the simulation of R_0 assuming the specified parameter is constant.

If we assume that the infected snail's mortality, or mortality rate of the *cercariae* are constant then, thermal optimum shifts to the right by 1.4°C at 26.9 ◦C. If we assume that the cercarial shedding rate is constant, the optimal temperature shifts toward lower temperatures by 1.7°C is at the lowest value (23.8 ◦C) and shift occurs toward the left.

Table 2: The table shows the magnitude and direction of shift for optimal temperature when we assume the corresponding parameter constant.

Parameter	**The shift in opt. temp. (New Opt. temp.)**	**The direction**
Infected snails' mortality rate $\mu_i(T)$	1.4 ◦ C (26.9 ◦ C)	Right
Miracidia's mortality rate $\mu_m(T)$	0.9 ◦ C (26.4 ◦ C)	Right
The mortality rate of the cercaria $\mu_c(T)$	1.4 ◦ C (26.9 ◦ C)	Right
The Probability of hatching success of *miracidia* $\delta_e(T)$	0.5 ◦ C (25 ◦ C)	Left
Snails' prepatent period $\sigma_S(T)$	0.7 ◦ C (24.8 ◦ C)	Left
The number of cercariae released $\nu_c(T)$	1.7 ◦ C (23.8 ◦ C)	Left
The transmission rate of schistosomiasis in the snails $\beta_s(T)$	1.6 ◦ C (23.9 ◦ C)	Left
The transmission rate of schistosomiasis in humans $\beta_h(T)$	0.3 ◦ C (25.2 ◦ C)	Left

Thermal response of transmission with human water contact rate

We found that thermal optimum further shifts toward higher temperatures when we accounted for the temperature-dependence of the water contact rate (**Figure 5**B-C). We found that the steepness and T_{med} determine the direction and intensity of the shift. Specifically, we observed a shift to the right larger than 1 °C in the thermal response curve of R_0 (**Figure 5**B) and a shift to the right of about 1 °C in the prevalence in human (**Figure 5**C). This analysis was performed only for the *S. mansoni-Biomphalaria* spp. system, as more data were available for TPC estimation than for *S. mansoni-Biomphalaria* spp.

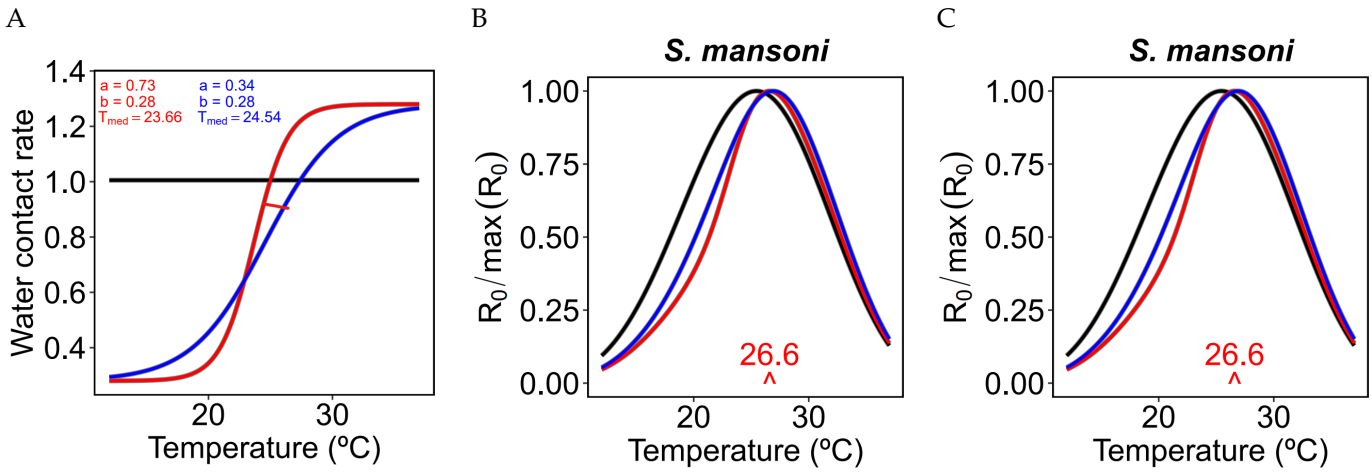

Figure 5: Effect of a temperature-dependent water contact rate on model results. (A) Water contact rate as a function of temperature for different values of the parameters in equation (9). The red line is the sigmoid function with the frequency of water contact data for two years of records in a village near the Senegal River given by *[46]*. The effect on R_0 and prevalence in humans are shown in **(B)** and **(C)**.

4. Discussion

We parameterized a detailed mechanistic, process-based, thermal sensitive model accounting for the complex life cycle of *Schistosoma* parasites with the results of an extensive literature review on the thermal tolerance of snail and parasite life history traits for *S. mansoni* and *S. haematobium*, which in this context have not been studied separately. We found that the thermal optimum for the basic reproduction number R_0 is remarkably higher than previously estimated.

According to our analysis, the reproduction number R_0 peaks at 25.5 and 26.2 °C for *S. mansoni* and *S. haematobium*, respectively (**Figure 3**A-B). As we accounted for the uncertainty of model outcomes, we found the 95% credible intervals

of optimal temperature are [23.1, 27.3] and [23.6, 27.9] °C for *S. mansoni* and *S. haematobium*. Interestingly, our finding indicates the thermal optima for R_0 and for the prevalence of infection in humans are not perfectly overlapping. These thermal optima are 4 degrees higher and even our lower bounds of 95th credible intervals are higher than the previous estimation, 21.7 °C (95% CI 20.5, 23.1), by [25]. The model presented here differs in many details, for instance including a state variable for prepatent snails and accounting for the temperature-dependent incubation period of snails. More precisely, the incubation period decreases by 80% and 75% for *Biomphalaria* and *Bulinus* species, respectively, between 15 and 35 °C (

Figure 2 : Thermal performance curves for temperature-dependent parameters. Inset panels show the thermal curve for a subset of temperatures on a zoomed-in y-axis. Different colors are used for different data sources.

We used the Euler-Lotka equation to derive the fecundity rate of *Biomphalaria* and *Bulinus* snails (**Error! Reference source not found.**A and B), respectively, from snails' egg laying, hatching, survival, and maturation rates (SM). Separate thermal curves for each of these processes are available in the SM. We found the best-fit function for fecundity rate for *Biomphalaria* spp. (*B. pfeifferi, B. alexandrina, B. glabrata, B. sudanica* is a concave unimodal shape that peaks at 24 ◦C, with lower (T_{min}) and upper (T_{max}) critical thermal thresholds at ~14 and 33°C, respectively. On the other hand, the best fit for *Bulinus* spp. (*B. globosus, B. truncatus, B. nyassanus*) fecundity data is a Johnson Lewin curve with a peak close to 28 ◦ T_{min} ,T_{max} around 10 and 32 ◦C, respectively. These peak temperatures are higher than the previous estimate (22.1 ◦ C) for all *Biomphalaria* and *Bulinus* spp. combined. Overall, we found *Bulinus* spp. to have a lower fecundity rate than *Biomphalaria* spp., with *Biomphalaria alexandrina* having the lowest fecundity rate among *Biomphalaria* spp. (see SM). We also observed that the confidence interval around the fecundity rate TPC for *Biomphalaria* spp. is narrower than for *Bulinus* spp. (Figure S1B-S2B).

The mortality rates of snails (**Error! Reference source not found.**C and 2D) are calculated from the fraction of snail surviving during each laboratory experiment at a given temperature. The best fit for *Biomphalaria* spp. (*B. pfeifferi, B. alexandrina, B. sudanica*) is a unimodal convex curve (Spain) [55] with a minimum at 21 ◦C. The best fit for *Bulinus* spp. (*B. globosus, B. truncatus, B. africanus, B. nyassanus*) is a quadratic function [56] with a minimum close to 15 ◦C. The empirical data show that mortality increases rapidly at high temperatures. The best fit across the entire temperature range accounted for in this study was obtained by using two curves, one for temperatures below 33 ◦C (**Error! Reference source not found.**C and D, inset panels) and the other for temperatures above 33 ◦C. We observed lower variability for *Biomphalaria* spp. than *Bulinus* spp. in the confidence intervals around the TPC for the snail's mortality rate (Figure S3B-S4B).

The mortality rates of infected snails were calculated from the snails' survival time at different temperatures after exposure to *miracidia* (**Error! Reference source not found.**E and 2F). The best-fit curves for *Biomphalaria* spp. (*B. glabrata, B. pfeifferi*) and *Bulinus* spp. (*B. globosus, B. truncatus*) are Flinn [57] and Spain [55], respectively. Mortality rates increase as temperature increases both for *Biomphalaria* spp. infected with *S. mansoni* and for *Bulinus* spp. infected with *S. haematobium*. As for the natural mortality rate of snails, we fitted the curves for mortality rate iof infected snails to data for higher and lower temperatures separately (**Error! Reference source not found.**E and 2F inset panels). We observe strong noise in the data, particularly for *Biomphalaria* spp., and wider confidence intervals at higher temperatures (Figure S12B-S13B).

The prepatent period, the average time between snail infection with *miracidia* and the onset of cercarial shedding (**Error! Reference source not found.**G and H), is best fit by a declining tail of a Gaussian function of temperature for both *Biomphalaria* spp. (*B. glabrata, B. pfeifferi*) and *Bulinus* spp. (*B. truncatus, B. globosus*) (Figure S5B-S6B) [58]. Data show little variability in prepatent time among snails of the same genus, and that *Bulinus* snails have a longer prepatent time than *Biomphalaria* snails (**Error! Reference source not found.**G and H).

The mortality rate of *miracidia* is calculated from their survival time at different temperatures (**Error! Reference source not found.**I and J). The best-fit curve is Thomas [59] for *S. mansoni*, with the lowest mortality rate at 13.5 ◦C, and Spain [55] for *S.haematobium*, with the lowest mortality rate occurring at 22.5 ◦C. We found strong noise in the confidence interval around the TPC at high and low temperatures for *S. mansoni*. We could not calculate the confidence intervals around the TPC of *S. haematobium* through bootstrapping due to the small size of the dataset. In this case, we generated a confidence interval by resampling from the confidence interval of the estimated TPC parameters. The mortality rate of *cercariae* (**Error! Reference source not found.**P) is also calculated from the proportion of surviving larvae at different temperatures. The best-fit curve for the data is Spain [55], with the lowest mortality of *cercariae* at 16.5 ◦C.

We observe a rapid increase at high temperatures, with narrow confidence intervals around TPC (Figure S9B-S10B-S11B).

The transmission rate from *miracidia* to snails (**Error! Reference source not found.**K and L) was estimated by utilizing a mechanistic model from data on the percentage of infected *Biomphalaria* spp. (*B. glabrata, B. pfeifferi*) and *Bulinus* spp. (*B. globosus, B. trancatus*) following exposure to *S. mansoni* and *S. haematobium* respectively (see SM). The best-fit curves are Spain [55] for *Biomphalaria* spp. exposed to *S. mansoni* and Flinn [57] for *Bulinus* spp. exposed to *S. haematobium*. Transmission rate peaked at 33 ◦C for *Biomphalaria* spp. and 30.5 ◦C for *Bulinus* spp. The transmission rate from *cercariae* to humans (**Error! Reference source not found.**M) is estimated from a separate SIR model of mice and cercaria by using the data of infection rate. Experimental studies are only available for *S. mansoni.* The best-fit function for this data is a Brière curve [60], with an optimal temperature for transmission around 24.5 ◦C. We observe transmission happening at as low as 10 ◦C and as high as 40 ◦C. Due to different laboratory conditions, both the miracidium-to-snail and the cercaria-to-human transmission rates have strong noise in the data and wide confidence intervals (Figure S14B-S15B-S16B).

The hatching probability of *miracidia* (**Error! Reference source not found.**N) is evaluated as the proportion of *miracidia* successfully hatching. Only one study was found measuring this parameter and it focused on *S. mansoni*. The best-fit function for these data is Flinn [57], showing a monotonic increase with temperature. Uncertainty increases with temperature (Figure S7B). The number of *cercariae* released per day by one snail (**Error! Reference source not found.**O) was obtained from two empirical studies of *Biomphalaria* spp. infected by *S. mansoni*. Based on these two studies, the best-fit function is a Gaussian curve [58], with its peak at 27.5 ◦C, matching finding in [25], and T_{min}, T_{max} are 10 and 40 ◦C, respectively. The confidence interval around the TPC becomes wider at higher temperatures (Figure S8B).

Table 1: Summary of temperature-dependent parameter shows the shape of curve, resources of data, location in the figure panel and optimal temperature with 95 percent credible interval for each corresponding parameter.G-H), therefore this parameter clearly affects the thermal performance of schistosomiasis transmission. This large decrease in the length of the prepatent period at high temperature may account for the higher thermal optimum produced by our model. In addition, we found multiple empirical studies [26,27,66] on the thermal response of snails' egg production, hatching, survival and maturation rates, which consistently show no egg reproduction at high temperatures. We account for these temperature-dependent snail LHTs in the snail fecundity rate in our model, which leads to a higher optimal temperature for R_0 as well. In addition, the GNTD data on human schistosomiasis prevalence in the field suggest that *S. haematobium* may have a larger thermal breadth than *S. mansoni* (**Figure 3**C-D); our model projections better fit this observation. A higher thermal optimum has implications for the response of schistosomiasis to climate change [4,67–69]. The average temperature in many countries currently affected by schistosomiasis is 22-30 °C [68] and thus the response of schistosomiasis to warming depends on whether temperature increases to approach or exceed the thermal optimum.

Although our model encompasses many aspects of schistosomiasis transmission, the complexity of the parasite's life cycle, the variability of LHTs across different species, and the low data availability limit our ability to fully explain the thermal dependence of schistosomiasis transmission. The prevalence of schistosomiasis from GNTD data bases revealed a high variability across the temperature that is not fully captured by our mechanistic model. There are many ecological, environmental, and human and snail behavioral factors that influence transmission, which we do not consider here, and which could contribute to that variability. Our model did not account for behavioral responses of snails to heat waves, such as diving deeper in search of temperature refugia, or entering an hypobiotic state (aestivation) by digging into the mud, which is a strategy observed for instance in the case of *Bulinus* spp. Snails (add reference regarding estivation). Future analysis should account for the possibility of thermal refugia, overwintering and estivation.

On the contrary, possible human behavioral responses like, for instance, increasing contact rates with water at higher temperatures, further shifts the thermal optimum for both R_0 and prevalence in humans. Another example could be favorable conditions for the snail reproduction rate, such as the availability of vegetation that serves as habitat. These are only a few examples of environmental conditions that may affect schistosomiasis transmission and highlights that models will always be limited by the mechanisms they choose to include or exclude.

As in most infectious disease systems, the availability of empirical observations in controlled field or laboratory settings to estimate TPCs for key demographic and epidemiological parameters is a key limitation to the projection power of mechanistic, process-based models of schistosomiasis transmission. Temperature-dependent trait data from laboratory studies were most readily available for the *S. mansoni-Biomphalaria* spp. system and were more limited for the *S. haematobium* and *Bulinus* spp. system. Some of the experiments used in the present study were conducted nearly 90 years ago, and more recent updates are urgently needed to dissect the temperature sensitivity of transmission for different schistosome species and snail hosts.

Although we used all the data, we have been able to retrieve for the parameterization of temperature dependence in both schistosomes and snails, our study still has some data limitations. For instance, to offset the paucity of data over a large thermal breadth, we had to pool together snail data from the same genus, but different species. When data were simply not available, as in the case of the *cercariae* release rate, the *cercariae* mortality rate, the hatching rate of *miracidia*, and the transmission rate in humans for the *S. haematobium-Bulinus* spp. system, we used TPCs estimated for the S. *mansoni-Biomphalaria* spp. system [6]. Therefore, our projection for the *S. haematobium-Bulinus* spp. system is inevitably biased by this choice. Further empirical studies are needed to derive TPCs for all the relevant parameters and the specific snails of public health importance. More specifically, mortality rate of cercaria and *miracidia* and transmission rate in humans for *S. haematobium.* An additional challenge of our study in the fitting process is the strong noise, which causes uncertainty in the fitted curves. Additional laboratory and modeling work will thus be needed to elucidate the thermal response of different snail species.

We also derive the thermal response of the basic reproduction number Ro under the assumption of constant temperatures. Therefore, the modelling approach presented here did not account for the effect of seasonal fluctuations, nor for daily and interannual variability of temperature [8,70]. For example, snails exhibit some behavioral responses to temperature variation like estivation and overwintering [41,71]. Future work should consider the dynamic impact of such variations in behavioral and physiological response to short term vs long term fluctuations in temperatures.

Further details, such as snail size [27] which can dramatically affect the thermal response of schistosomiasis, should also be taken into account. Finally, we focus here on temperature as the primary influencing factor in our model. The proposed disease transmission-related dynamics are likely realistic over a broad geographic scale, but several other socioeconomic (poverty, access to clean water, etc.), behavioral, climatic (such as precipitation) and environmental (water availability and water quality) factors drive these processes as well and will need to be considered to better understand and project how large-scale temperature change will impact schistosomiasis transmission.

5. Conclusions

Environmentally mediated diseases often have complex life cycles and may respond in complex and nonlinear ways to temperature change. Here, we built a temperature-sensitive model of schistosomiasis based on two common *Schistosoma* parasites in SSA and found a higher thermal optimum than previously estimated. These results are consistent with prevalence data across Africa and highlight the importance of high-quality and species-specific data on the temperature-dependence of LHTs to project the impact of climate change on disease transmission. Compared to the previous models, our model reveals a wider range of areas will be subject to warming-driven increases of transmission due to temperature suitability. We might observe higher prevalence of schistosomiasis in the countries of Southeast Africa like Zombie, Zimbabwe and even expansion in Botswana [72,73].

Acknowledgments: This work is funded by the Stanford Center for Innovation in Global Health, Belmont Forum on Climate Environment and Health, UKRI (UK), FAPESP (Brazil), PASRES (Côte d'Ivoire), and the USA National Science Foundation (DEB-2024383; DEB-2011147; DEB 2011179, Belmont CEH/NSF ICER-2024383). EAM was funded by the National Science Foundation (DEB-2011147 with Fogarty International Center), the National Institutes of Health (R35GM133439, R01AI168097, R01AI102918), and the Stanford Center for Innovation in Global Health and Woods Institute for the Environment. The authors are also particularly grateful to Dr. Penelope Vounatsou (Swiss TPH), the curator of the GNTD dataset.

Conflicts of Interest: "The authors declare no conflict of interest."

References

1. Arnell, N.W.; Lowe, J.A.; Challinor, A.J.; Osborn, T.J. Global and Regional Impacts of Climate Change at Different Levels of Global Temperature Increase. *Climatic Change* **2019**, *155*, 377–391, doi:10.1007/s10584-019-02464-z.
2. Walther, G.-R.; Post, E.; Convey, P.; Menzel, A.; Parmesan, C.; Beebee, T.J.; Fromentin, J.-M.; Hoegh-Guldberg, O.; Bairlein, F. Ecological Responses to Recent Climate Change. *Nature* **2002**, *416*, 389–395.
3. Cubasch, U.; Meehl, G.; Boer, G.; Stouffer, R.; Dix, M.; Noda, A.; Senior, C.; Raper, S.; Yap, K. Projections of Future Climate Change. In *Climate Change 2001: The scientific basis. Contribution of WG1 to the Third Assessment Report of the IPCC (TAR)*; Cambridge University Press, 2001; pp. 525–582.
4. Iyakaremye, V.; Zeng, G.; Zhang, G. Changes in Extreme Temperature Events over Africa under 1.5 and 2.0°C Global Warming Scenarios. *International Journal of Climatology* **2021**, *41*, 1506–1524, doi:10.1002/joc.6868.

5. Stensgaard, A.-S.; Vounatsou, P.; Sengupta, M.E.; Utzinger, J. Schistosomes, Snails and Climate Change: Current Trends and Future Expectations. *Acta tropica* **2019**, *190*, 257–268.
6. Mordecai, E.A.; Paaijmans, K.P.; Johnson, L.R.; Balzer, C.; Ben-Horin, T.; de Moor, E.; McNally, A.; Pawar, S.; Ryan, S.J.; Smith, T.C.; et al. Optimal Temperature for Malaria Transmission Is Dramatically Lower than Previously Predicted. *Ecology Letters* **2013**, *16*, 22–30, doi:10.1111/ele.12015.
7. Paaijmans, K.P.; Heinig, R.L.; Seliga, R.A.; Blanford, J.I.; Blanford, S.; Murdock, C.C.; Thomas, M.B. Temperature Variation Makes Ectotherms More Sensitive to Climate Change. *Global change biology* **2013**, *19*, 2373–2380.
8. Paaijmans, K.P.; Blanford, S.; Bell, A.S.; Blanford, J.I.; Read, A.F.; Thomas, M.B. Influence of Climate on Malaria Transmission Depends on Daily Temperature Variation. *Proceedings of the National Academy of Sciences* **2010**, *107*, 15135–15139, doi:10.1073/pnas.1006422107.
9. Kalinda, C.; Chimbari, M.; Mukaratirwa, S. Implications of Changing Temperatures on the Growth, Fecundity and Survival of Intermediate Host Snails of Schistosomiasis: A Systematic Review. *International Journal of Environmental Research and Public Health* **2017**, *14*, 80.
10. Kalinda, C.; Mutengo, M.; Chimbari, M. A Meta-Analysis of Changes in Schistosomiasis Prevalence in Zambia: Implications on the 2020 Elimination Target. *Parasitology research* **2020**, *119*, 1–10.
11. Hailegebriel, T.; Nibret, E.; Munshea, A. Prevalence of Schistosoma Mansoni and S. Haematobium in Snail Intermediate Hosts in Africa: A Systematic Review and Meta-Analysis. *Journal of tropical medicine* **2020**, *2020*.
12. Yang, G.-J.; Utzinger, J.; Sun, L.-P.; Hong, Q.-B.; Vounatsou, P.; Tanner, M.; Zhou, X.-N. Effect of Temperature on the Development of Schistosoma Japonicum within Oncomelania Hupensis, and Hibernation of O. Hupensis. *Parasitology Research* **2007**, *100*, 695–700.
13. Gordon, R.; Davey, T.; Peaston, H. The Transmission of Human Bilharziasis in Sierra Leone, with an Account of the Life-Cycle of the Schistosomes Concerned, S. Mansoni and S. Haematobium. *Annals of Tropical Medicine & Parasitology* **1934**, *28*, 323–418.
14. Anderson, R.M.; Mercer, J.G.; Wilson, R.A.; Carter, N.P. Transmission of *Schistosoma Mansoni* from Man to Snail: Experimental Studies of Miracidial Survival and Infectivity in Relation to Larval Age, Water Temperature, Host Size and Host Age. *Parasitology* **1982**, *85*, 339–360, doi:10.1017/S0031182000055323.
15. Prah, S.; James, C. The Influence of Physical Factors on the Survival and Infectivity of Miracidia of Schistosoma Mansoni and S. Haematobium I. Effect of Temperature and Ultra-Violet Light. *Journal of Helminthology* **1977**, *51*, 73–85.
16. Purnell, R. Host-Parasite Relationships in Schistosomiasis: III.—The Effect of Temperature on the Survival of Schistosoma Monsoni Miracidia and on the Survival and Infectivity of Schistosoma Mansoni Cercariae. *Annals of Tropical Medicine & Parasitology* **1966**, *60*, 182–186.
17. Shiff, C. Seasonal Factors Influencing the Location of Bulinus (Physopsis) Globosus by Miracidia of Schistosoma Haematobium in Nature. *The Journal of parasitology* **1974**, 578–583.
18. Chu, K.; Massoud, J.; Sabbaghian, H. Host-Parasite Relationship of Bulinus Truncatus and Schistosoma Haematobium in Iran: 3. Effect of Water Temperature on the Ability of Miracidia to Infect Snails. *Bulletin of the World Health Organization* **1966**, *34*, 131.
19. Foster, R.; others The Effect of Temperature on the Development of Schistosoma Mansoni Sambon 1907 in the Intermediate Host. *Journal of Tropical Medicine and Hygiene* **1964**, *67*, 289–292.
20. Stirewalt, M.A. Effect of Snail Maintenance Temperatures on Development of Schistosoma Mansoni. *Experimental Parasitology* **1954**, *3*, 504–516.
21. DeWitt, W.B. Influence of Temperature on Penetration of Snail Hosts by Schistosoma Mansoni Miracidia. *Experimental Parasitology* **1955**, *4*, 271–276.

22. Coelho, J.R.; Bezerra, F.S. The Effects of Temperature Change on the Infection Rate of Biomphalaria Glabrata with Schistosoma Mansoni. *Memórias do Instituto Oswaldo Cruz* **2006**, *101*, 223–224.
23. Upatham, E.S.; others The Effect of Water Temperature on the Penetration and Development of St. Lucian Schistosoma Mansoni Miracidia in Local Biomphalaria Glabrata. *Southeast Asian J Trop Med Public Health* **1973**, *4*, 367–370.
24. Lawson, J.R.; Wilson, R. The Survival of the Cercariae of Schistosoma Mansoni in Relation to Water Temperature and Glycogen Utilization. *Parasitology* **1980**, *81*, 337–348.
25. Nguyen, K.H.; Boersch-Supan, P.H.; Hartman, R.B.; Mendiola, S.Y.; Harwood, V.J.; Civitello, D.J.; Rohr, J.R. Interventions Can Shift the Thermal Optimum for Parasitic Disease Transmission. *Proceedings of the National Academy of Sciences* **2021**, *118*, e2017537118.
26. Sturrock, R. The Influence of Temperature on the Biology of Biomphalaria Pfeifferi (Krauss), an Intermediate Host of Schistosoma Mansoni. *Annals of Tropical Medicine & Parasitology* **1966**, *60*, 100–105.
27. El-Hassan, A.A. Laboratory Studies on the Direct Effect of Temperature on Bulinus Truncatus and Biomphalaria Alexandrina, the Snail Intermediate Hosts of Schistosomes in Egypt. *Folia Parasitol (Praha)* **1974**, *21*, 181–187.
28. Appleton, C.C. The Influence of Temperature on the Life-Cycle and Distribution of Biomphalaria Pfeifferi (Krauss, 1948) in South-Eastern Africa. *International Journal for Parasitology* **1977**, *7*, 335–345, doi:10.1016/0020-7519(77)90057-1.
29. CHEEVER, A.; MACEDONIA, J. MOSHMANN. 1 E. & CHEEVER, EA-Kinetics of Egg Production and Egg Excretion by Schistosoma Mansoni and Schistosoma Japonicum in Mice Infected with a Single Pair of Worms. Amcr. *J. trop. Med. Hyg* **1994**, *50*, 281–295.
30. Shiff, C. Studies on Bulinus (Physopsis) Globosus in Rhodesia. *Annalsof Tropical Medicine & Parasitology* **1964**, *58*.
31. Michelson, E.H.; others The Effects of Temperature on Growth and Reproduction of Australorbis Glabratus in the Laboratory. *American Journal of Hygiene* **1961**, *73*, 66–74.
32. Kubirizajournal, G.K.; Madsen, H.; Likongwe, J.S.; Stauffer Jr, J.R.; OmbeJeremiah, K.褒; Kapute, F. Effect of Temperature on Growth, Survival and Reproduction of Bulinus Nyassanus (Smith, 1877)(Mollusca: Gastropoda) from Lake Malawi. *African Zoology* **2010**, *45*, 315–320.
33. Pfluger, W. Experimental Epidemiology of Schistosomiasis. *Zeitschrift fur Parasitenkunde* **1981**, *63*.
34. Pflüger, W. Experimental Epidemiology of Schistosomiasis: I. The Prepatent Period and Cercarial Production of Schistosoma Mansoni in Biomphalaria Snails at Various Constant Temperatures. *Zeitschrift für Parasitenkunde* **1980**, *63*, 159–169.
35. Brauer, F.; Castillo-Chavez, C. *Mathematical Models in Population Biology and Epidemiology*; Texts in Applied Mathematics; Springer: New York, NY, 2012; Vol. 40; ISBN 978-1-4614-1685-2.
36. Keeling, M.; Rohani, P. Modeling Infectious Diseases in Humans and Animals Princeton Univ. *Princeton, NJ* **2008**.
37. Mangal, T.D.; Paterson, S.; Fenton, A. Predicting the Impact of Long-Term Temperature Changes on the Epidemiology and Control of Schistosomiasis: A Mechanistic Model. *PLoS one* **2008**, *3*, e1438.
38. McCreesh, N.; Booth, M. The Effect of Increasing Water Temperatures on Schistosoma Mansoni Transmission and Biomphalaria Pfeifferi Population Dynamics: An Agent-Based Modelling Study. *PLoS One* **2014**, *9*, e101462.
39. Kalinda, C.; Mushayabasa, S.; Chimbari, M.J.; Mukaratirwa, S. Optimal Control Applied to a Temperature Dependent Schistosomiasis Model. *Biosystems* **2019**, *175*, 47–56.
40. Gao, S.; Liu, Y.; Luo, Y.; Xie, D. Control Problems of a Mathematical Model for Schistosomiasis Transmission Dynamics. *Nonlinear Dynamics* **2011**, *63*, 503–512.

41. Huang, Q.; Gurarie, D.; Ndeffo-Mbah, M.; Li, E.; King, C.H. Schistosoma Transmission in a Dynamic Seasonal Environment and Its Impact on the Effectiveness of Disease Control. *The Journal of Infectious Diseases* **2022**, *225*, 1050–1061.
42. Ciddio, M.; Mari, L.; Gatto, M.; Rinaldo, A.; Casagrandi, R. The Temporal Patterns of Disease Severity and Prevalence in Schistosomiasis. *Chaos* **2015**, *25*, 036405, doi:10.1063/1.4908202.
43. Le Clec'h, W.; Diaz, R.; Chevalier, F.D.; McDew-White, M.; Anderson, T.J.C. Striking Differences in Virulence, Transmission and Sporocyst Growth Dynamics between Two Schistosome Populations. *Parasites & Vectors* **2019**, *12*, 485, doi:10.1186/s13071-019-3741-z.
44. Le, T.-L.; Sokolow, S.H.; Hammam, O.; Fu, C.-L.; Hsieh, M. Pathogenesis of Human Schistosomiasis. In *Human Emerging and Re-emerging Infections*; John Wiley & Sons, Ltd, 2015; pp. 481–504 ISBN 978-1-118-64484-3.
45. Gurarie, D.; Lo, N.C.; Ndeffo-Mbah, M.L.; Durham, D.P.; King, C.H. The Human-Snail Transmission Environment Shapes Long Term Schistosomiasis Control Outcomes: Implications for Improving the Accuracy of Predictive Modeling. *PLoS neglected tropical diseases* **2018**, *12*, e0006514.
46. Sow, S.; de Vlas, S.J.; Stelma, F.; Vereecken, K.; Gryseels, B.; Polman, K. The Contribution of Water Contact Behavior to the High Schistosoma Mansoni Infection Rates Observed in the Senegal River Basin. *BMC infectious diseases* **2011**, *11*, 1–11.
47. Daniel, P.; Hannah, O. rTPC: Functions for Fitting Thermal Performance Curves.
48. Wood, C.L.; Sokolow, S.H.; Jones, I.J.; Chamberlin, A.J.; Lafferty, K.D.; Kuris, A.M.; Jocque, M.; Hopkins, S.; Adams, G.; Buck, J.C.; et al. Precision Mapping of Snail Habitat Provides a Powerful Indicator of Human Schistosomiasis Transmission. *Proceedings of the National Academy of Sciences* **2019**, *116*, 23182–23191.
49. Sokolow, S.H.; Huttinger, E.; Jouanard, N.; Hsieh, M.H.; Lafferty, K.D.; Kuris, A.M.; Riveau, G.; Senghor, S.; Thiam, C.; N'Diaye, A.; et al. Reduced Transmission of Human Schistosomiasis after Restoration of a Native River Prawn That Preys on the Snail Intermediate Host. *Proceedings of the National Academy of Sciences* **2015**, *112*, 9650–9655.
50. Jones, I.J.; Sokolow, S.H.; Chamberlin, A.J.; Lund, A.J.; Jouanard, N.; Bandagny, L.; Ndione, R.; Senghor, S.; Schacht, A.-M.; Riveau, G.; et al. Schistosome Infection in Senegal Is Associated with Different Spatial Extents of Risk and Ecological Drivers for Schistosoma Haematobium and S. Mansoni. *PLOS Neglected Tropical Diseases* **2021**, *15*, e0009712, doi:10.1371/journal.pntd.0009712.
51. Dietz, K. The Estimation of the Basic Reproduction Number for Infectious Diseases. *Stat Methods Med Res* **1993**, *2*, 23–41, doi:10.1177/096228029300200103.
52. Heesterbeek, J.A.P. A Brief History of R 0 and a Recipe for Its Calculation. *Acta biotheoretica* **2002**, *50*, 189–204.
53. May, R.M. Togetherness among Schistosomes: Its Effects on the Dynamics of the Infection. *Mathematical Biosciences* **1977**, *35*, 301–343, doi:10.1016/0025-5564(77)90030-X.
54. Johnson, F.H.; Lewin, I. The Growth Rate of E. Coli in Relation to Temperature, Quinine and Coenzyme. *Journal of Cellular and Comparative Physiology* **1946**, *28*, 47–75.
55. Cunningham, P. Basic Microcomputer Models in Biology: By James D. Spain Addison-Wesley; Reading MA, 1982 Xiv+ 354 Pages. $23.50;\pounds 15.50 1983.
56. Montagnes, D.J.; Morgan, G.; Bissinger, J.E.; Atkinson, D.; Weisse, T. Short-Term Temperature Change May Impact Freshwater Carbon Flux: A Microbial Perspective. *Global Change Biology* **2008**, *14*, 2823–2838.
57. Flinn, P. Temperature-Dependent Functional Response of the Parasitoid Cephalonomia Waterstoni (Gahan)(Hymenoptera: Bethylidae) Attacking Rusty Grain Beetle Larvae (Coleoptera: Cucujidae). *Environmental Entomology* **1991**, *20*, 872–876.
58. Lynch, M.; Gabriel, W. Environmental Tolerance. *The American Naturalist* **1987**, *129*, 283–303.

59. Thomas, M.K.; Aranguren-Gassis, M.; Kremer, C.T.; Gould, M.R.; Anderson, K.; Klausmeier, C.A.; Litchman, E. Temperature–Nutrient Interactions Exacerbate Sensitivity to Warming in Phytoplankton. *Global change biology* **2017**, *23*, 3269–3280.
60. Briere, J.-F.; Pracros, P.; Le Roux, A.-Y.; Pierre, J.-S. A Novel Rate Model of Temperature-Dependent Development for Arthropods. *Environmental Entomology* **1999**, *28*, 22–29.
61. McCreesh, N.; Arinaitwe, M.; Arineitwe, W.; Tukahebwa, E.M.; Booth, M. Effect of Water Temperature and Population Density on the Population Dynamics of Schistosoma Mansoni Intermediate Host Snails. *Parasites & Vectors* **2014**, *7*, 1–9.
62. Shiff, C. The Influence of Temperature on the Intrinsic Rate of Naturol Increase of the Freshwater Snail, Biomphalaria Pfeifferi (Krauss)(Pulmonata: Planorbidae). *Arch. Hydrobiol* **1967**, *62*, 429–438.
63. El-Emam, M.; Madsen, H. The Effect of Temperature, Darkness, Starvation and Various Food Types on Growth, Survival and Reproduction of Helisoma Duryi, Biomphalaria Alexandrina and Bulinus Truncatus (Gastropoda: Planorbidae). *Hydrobiologia* **1982**, *88*, 265–275.
64. Joubert, P.; Pretorius, S.; De Kock, K.; Van Eeden, J. Survival of Bulinus Africanus (Krauss), Bulinus Globosus (Morelet) and Biomphalaria Pfeifferi (Krauss) at Constant High Temperatures. *African Zoology* **1986**, *21*, 85–88.
65. Pflüger, W.; Roushdy, M.; Emam, M.E. The Prepatent Period and Cercarial Production of Schistosoma Haematobium in Bulinus Truncatus (Egyptian Field Strains) at Different Constant Temperatures. *Zeitschrift für Parasitenkunde* **1984**, *70*, 95–103.
66. Sturrock, R.; Sturrock, B. The Influence of Temperature on the Biology of Biomphalaria Glabrata (Say), Intermediate Host of Schistosoma Mansoni on St. Lucia, West Indies. *Annals of Tropical Medicine & Parasitology* **1972**, *66*, 385–390.
67. Engelbrecht, F.; Adegoke, J.; Bopape, M.-J.; Naidoo, M.; Garland, R.; Thatcher, M.; McGregor, J.; Katzfey, J.; Werner, M.; Ichoku, C.; et al. Projections of Rapidly Rising Surface Temperatures over Africa under Low Mitigation. *Environ. Res. Lett.* **2015**, *10*, 085004, doi:10.1088/1748-9326/10/8/085004.
68. Engdaw, M.M.; Ballinger, A.P.; Hegerl, G.C.; Steiner, A.K. Changes in Temperature and Heat Waves over Africa Using Observational and Reanalysis Data Sets. *International Journal of Climatology* **2022**, *42*, 1165–1180, doi:10.1002/joc.7295.
69. Babaousmail, H.; Ayugi, B.O.; Ojara, M.; Ngoma, H.; Oduro, C.; Mumo, R.; Ongoma, V. Projection of the Diurnal Temperature Range over Africa Based on CMIP6 Simulations. *Journal of African Earth Sciences* **2023**, *200*, 104883, doi:10.1016/j.jafrearsci.2023.104883.
70. Lambrechts, L.; Paaijmans, K.P.; Fansiri, T.; Carrington, L.B.; Kramer, L.D.; Thomas, M.B.; Scott, T.W. Impact of Daily Temperature Fluctuations on Dengue Virus Transmission by Aedes Aegypti. *Proceedings of the National Academy of Sciences* **2011**, *108*, 7460–7465, doi:10.1073/pnas.1101377108.
71. Rubaba, O.; Chimbari, M.; Mukaratirwa, S. The Role of Snail Aestivation in Transmission of Schistosomiasis in Changing Climatic Conditions. *African Journal of Aquatic Science* **2016**, *41*, 143–150, doi:10.2989/16085914.2016.1145103.
72. Wanders, N.; van Vliet, M.T.H.; Wada, Y.; Bierkens, M.F.P.; van Beek, L.P.H. (Rens) High-Resolution Global Water Temperature Modeling. *Water Resources Research* **2019**, *55*, 2760–2778, doi:10.1029/2018WR023250.
73. Statistics and Data of All Countries in Africa Available online: https://www.worlddata.info/africa/index.php (accessed on 25 November 2023).

Disclaimer/Publisher's Note: The statements, opinions and data contained in all publications are solely those of the individual author(s) and contributor(s) and not of MDPI and/or the editor(s). MDPI and/or the editor(s) disclaim responsibility for any injury to people or property resulting from any ideas, methods, instructions or products referred to in the content.